

Manuscript Number: MAGMA-D-13-01129R1

Title: Magnetism Variations and Susceptibility Hysteresis at the Metal-Insulator Phase Transition Temperature of VO<sub>2</sub> in a Composite Film Containing Vanadium and Tungsten Oxides

Article Type: Regular Submission

Corresponding Author: Dr. Bonex Wakufwa Mwakikunga, PhD

Corresponding Author's Institution: Council for Scientific and Industrial Research

First Author: Bonex Wakufwa Mwakikunga, PhD

Order of Authors: Bonex Wakufwa Mwakikunga, PhD; Amos A Akande, MSc; Erasmus K Rammutla, PhD(Physics); Thomas Moyo, PhD; Nadir S Osman, MSc; Steven S Nkosi, MSc; Charl Jafta, PhD

Abstract: We report on the magnetic property of 0.67-WO<sub>3</sub> + 0.33-VO<sub>x</sub> mixture film deposit on the corning glass substrate using chemical sol gel and atmospheric pressure chemical vapour deposition (APCVD) methods. The XRD and Raman spectroscopy confirm species of both materials, and the morphological studies with FIB-SEM and TEM reveal segregation of W and V atoms. XPS reveals that V<sup>4+</sup> from VO<sub>2</sub> forms only 11% of the film; V<sup>3+</sup> in the form of V<sub>2</sub>O<sub>3</sub> form 1% of the film, 21% is V<sup>5+</sup> from V<sub>2</sub>O<sub>5</sub> and 67% is given to W<sup>6+</sup> from WO<sub>3</sub>. The analysis of the ESR data shows some sharp changes in the magnetism near the MIT, which could be theoretically interpreted as the ordering or alignment of electron spins from net moment nature to parallel alignment of magnetic moment. The derivatives of magnetic susceptibility established the thermally induced magnetic property:- two distinct transitions of 339 K for heating data and 338 K for cooling data for 151.2 mT field were obtained. Similar results were also obtained for 308.7 mT field, 336 K for heating data and 335 K for cooling data. VSM results confirm a paramagnetic phase with a small amount of magnetically ordered phase.

DST/CSIR National Centre for Nano-Structured Materials, PO Box 395,  
Pretoria 0001, South Africa

To: Editor, Journal of Magnetism and Magnetic Materials

Attention to: Prof S Bader

Date: 22<sup>nd</sup> July, 2014

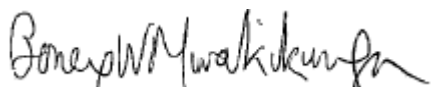
Dear Editor

Subject: **Re-vision and re-submission of article “Magnetism Variations and Susceptibility Hysteresis at the Metal-Insulator Phase Transition Temperature of VO<sub>2</sub> in a Composite Containing Vanadium and Tungsten Oxides”**

On behalf of all authors, I am happy to submit the above revised manuscript to your journal. We confirm that the manuscript has been duly revised and all the suggestions made by the reviewer have been considered accordingly.

We look forward to your consideration to publish our paper.

Yours sincerely,



**Bonex Mwakikunga**, PhD(Wits 2009), MSc (Wits 2006), BEdSc(Hons) (Malawi 1994), BEdSc(Malawi 1992)

**Principal Research (Nano Physics)**

Contact: 012 841 3784 or Mobile 084 211 7844

Ms. Ref. No.: MAGMA-D-13-01129

Title: Paramagnetism and Susceptibility Hysteresis Near the Metal - Insulator Phase Transition Temperature of Heavily Tungsten-Doped Vanadium Dioxide  
Journal of Magnetism and Magnetic Materials

Dear Bonex,

The reviewer has now commented on your paper. You will see that he/she is advising that you revise your manuscript. If you are prepared to undertake the work required, I would be pleased to reconsider my decision.

For your guidance, the reviewer's comments are appended below.

If you decide to revise the work, please submit a list of changes or a rebuttal against each point which is being raised when you submit the revised manuscript. Your revised manuscript should be submitted within one month. If you do not do so, we will assume that you do not wish to submit a revised version and your manuscript will be withdrawn from consideration.

To submit a revision, please go to <http://ees.elsevier.com/magma/> and login as an Author.

Your username is: [bmwakikunga@csir.co.za](mailto:bmwakikunga@csir.co.za)

If you need to retrieve password details, please go to:

[http://ees.elsevier.com/magma/automail\\_query.asp](http://ees.elsevier.com/magma/automail_query.asp)

NOTE: Upon submitting your revised manuscript, please upload the source files for your article. For additional details regarding acceptable file formats, please refer to the Guide for Authors at: <http://www.elsevier.com/journals/journal-of-magnetism-and-magnetic-materials/0304-8853/guide-for-authors>

When submitting your revised paper, we ask that you include the following items:

Manuscript and Figure Source Files (mandatory)

We cannot accommodate PDF manuscript files for production purposes. We also ask that when submitting your revision you follow the journal formatting guidelines. Figures and tables may be embedded within the source file for the submission as long as they are of sufficient resolution for Production. For any figure that cannot be embedded within the source file (such as \*.PSD Photoshop files), the original figure needs to be uploaded separately. Refer to the Guide for Authors for additional information.

<http://www.elsevier.com/journals/journal-of-magnetism-and-magnetic-materials/0304-8853/guide-for-authors>

Highlights (mandatory)

Highlights consist of a short collection of bullet points that convey the core findings of the article and should be submitted in a separate file in the online submission system. Please use 'Highlights' in the file name and include 3 to 5 bullet points (maximum 85 characters, including spaces, per bullet point). See the following website for more information

<http://www.elsevier.com/highlights>

Graphical Abstract (optional)

Graphical Abstracts should summarize the contents of the article in a concise, pictorial form designed to capture the attention of a wide readership online. Refer to the following website for more information:

<http://www.elsevier.com/graphicalabstracts>

On your Main Menu page is a folder entitled "Submissions Needing Revision". You will find your submission record there.

Please note that this journal offers a new, free service called AudioSlides: brief, webcast-style presentations that are shown next to published articles on ScienceDirect (see also <http://www.elsevier.com/audioslides>). If your paper is accepted for publication, you will automatically receive an invitation to create an AudioSlides presentation.

Yours sincerely,

Samuel D. Bader  
Editor  
Journal of Magnetism and Magnetic Materials

Reviewer's comments:

The article deals with observed magnetic property changes in heavily W-doped VO<sub>2</sub> sol-gel deposits, which is a topic of considerable interest to the VO<sub>2</sub> community. Materials characterization and ESR measurements were reported with due diligence. This paper should be published in JMMM only after the following points are addressed:

I have few main concerns, which if our authors can clarify/address, would be good:

- 1) The preparation and characterization of the deposit does not convince me if at all W-doping of VO<sub>2</sub> was achieved...from the TEMs in Fig.5 it is hard to say if there is a region where there is "VO<sub>2</sub>" doped with W...it is not very clear if the region that was scanned has VO<sub>2</sub> as well as W. Also, the amount of W-doping in percentage or concentration, which is necessary, has not been stated anywhere in the paper. The XRD in figure 3 can be taken by a large spot that encompasses both the "VO<sub>2</sub>" and the "W" areas next to each other. Same for the Raman Spectrum in figure 4. The hysteresis curves in figure 6 are generated only in the "VO<sub>2</sub>" area, hence leaving no scope for verifying the known fact that W-doping reduces the transition temperature of VO<sub>2</sub>. Hence, it hasn't been convincingly addressed if VO<sub>2</sub> has been successfully doped by W or not. Authors are requested to point out a proof of W-doping and provide a semi-quantitative estimate of how much W-incorporation has happened to make this study useful.

*Authors' response:* Thank you. The reviewer is correct. In order to verify the alleged W-doping, we have carried x-ray photoelectron spectroscopy (XPS). It is found that 67% of the film is W<sup>6+</sup> most likely from the WO<sub>3</sub> phase and then 33% is from vanadium oxides. Therefore this is not heavily W-doped film as we concluded before. This is equivalent to alloying. In fact the tungsten oxide phases separate themselves from the vanadium oxide phases in a process called segregation. XPS confirms Raman spectroscopy and XRD that WO<sub>3</sub> and V<sub>2</sub>O<sub>5</sub> seem to be predominant. We have presented XRD, Raman spectroscopy and XPS in Figure 3 of the revised manuscript and their discussion is on Page 13 and 14.

- 2) It is very important to make pure VO<sub>2</sub> to study the phase transition behavior. It seems like the sample in question had VO<sub>2</sub> (M1 as well as B) and V<sub>2</sub>O<sub>5</sub>, this makes the result interpretation a little complex. VO<sub>2</sub> (B) has been reported in literature to have a different transition temp. (see Corr et al, Journal of Materials Chemistry, 2009, 19, 4362-4367, and reference 8 and 9 in that paper, which refers to Oka et al - the magnetic property of VO<sub>2</sub>(B) has been reported in these as well.) Hence, the change of mag. property observed in this manuscript might not be attributable to W-doping.

*Authors' response:* Thank you again for this observation. Although this film has WO<sub>3</sub> and VO<sub>x</sub> phases, the 33% proportion ascribed to the VO<sub>x</sub> phases is further subdivided in accordance with XPS analysis as follows: 11% to VO<sub>2</sub> and 22% to V<sub>2</sub>O<sub>5</sub>. In the temperature range considered (300-353 K) only the VO<sub>2</sub> M<sub>1</sub> transition can be observed. The rest of the phases have transitions beyond this range; for instance VO<sub>2</sub> B or VO<sub>2</sub> A have transitions above 120 deg C (393 K) or 150 deg C (423K), WO<sub>3</sub> at 200 deg C (473 K), V<sub>2</sub>O<sub>5</sub> at 375 deg C (648K). This description is included in the revised manuscripts and indeed we have read and cited the suggested papers as follows:

Corr et al is already cited in Ref. 41

Ref [51] F. Theobald, R. Cabala, J. Bernard, Test on the structure of VO<sub>2</sub>(B), J. Solid State Chem., 17 (1976) 431

Ref [52] Y. Oka, T. Yao, N. Yamamoto, Y. Ueda, A. Hayashi, Phase transition and V<sup>4+</sup>-V<sup>4+</sup> pairing in VO<sub>2</sub>(B), J. Solid State Chem. 105 (1993) 271

- 3) The ESR data  $d\chi/dt$ , does not really tell us whether it is para, ferro or ferrimagnetic, it only indicates a change. We need the full susceptibility curve  $\chi(T)$  and M vs H hysteresis curve before and after transition to show that there is ferromagnetism after transition. Otherwise, the abstract and discussion needs to be modified to say only that, there is a change in magnetic susceptibility during transition, and it can be used to track the transition itself, as is correctly pointed out in the conclusion section.

Authors' response: The reviewer is correct. Some authors on ESR have ascribed sharp ESR line-shapes to para-magnetism and broad ESR line-shapes to ferro-magnetism []. This argument is based on the fact that ESR is in fact sometimes referred to as EPR (electron paramagnetic resonance) and therefore sharp and intense resonances are ascribed to para-magnetism. However other authors [] on ESR have explained sharp or broad as ferro or para respectively to the contrary; this difference in opinions shows that the use of the nature of the ESR line-shapes to ferro or ferri and para magnetism is not yet resolved in ESR.

In order to ascertain the para or ferro magnetism in this film, we have undertaken Vibrating Sample Magnetometry (VSM) in order to obtain M vs H hysteresis curves. We have obtained M vs H hysteresis curves from a commercial and pure VO<sub>2</sub> samples. Their degrees of para-magnetism and ferro-magnetism are now discussed on Page 16 of the revised manuscript and the results are presented in Fig 6 (c and d).

Title, introduction, references, figures and data presentation is satisfactory. The abstract, results and discussions sections need a little bit of work.

Title has slightly changes to reflect the corrections in the manuscript.

I would recommend this article for publication with certain revisions for enhancing the readability of this article:  
Thank you.

- 1) Section1: Page 4 , third paragraph, last sentence needs to be revised - optical probing generally give electronic information and not structural, and this sentence is not supported by any references either.  
Corrected, thank you.
- 2) There are some omitted words and grammatical mistakes in phrasing sentences all through the draft. If authors can please revise the draft accordingly that would be great. Some of them are pointed out here:  
Corrected, thank you.
  - a) Section 2.3: Last sentence missing the mathematical quantities.  
Corrected, thank you
  - b) Last paragraph in Section 4 before Conclusion which starts with Hysteresis in paramagnetic \_\_\_\_ (missing word) and susceptibility...". Next sentence : "One leads to the fact", Last sentence: crystallite "size" decrease - "size" word is missing.  
Corrected. Thank you.

Highlights for **Magnetism Variations and Susceptibility Thermal Hysteresis at the Metal-Insulator Phase Transition of VO<sub>2</sub> in Composite Containing Vanadium and Tungsten**

**Oxides** by A. A. Akande<sup>1, 2</sup>, K. E. Rammutla<sup>2</sup>, T. Moyo<sup>3</sup>, N. S-E. Osman<sup>3</sup>, S. S. Nkosi<sup>4</sup>, C. Jafta<sup>5</sup>,

B. W. Mwakikunga<sup>1,1</sup>

1. Variations in magnetism of VO<sub>2</sub> derived from electron spin resonance data at various temperatures is employed in observing the metal-to-insulator transition (MIT) temperature in VO<sub>2</sub>
2. Magnetization obtained from the inverse of the ESR intensity of the characteristic peaks in the field sweeps yields novel shapes of the hysteresis loops.
3. Susceptibility derived from the paramagnetic signature confirms the VO<sub>2</sub> MIT at 340 K.
4. Hysteresis loop width from susceptibility is just about 1 K whereas the conductivity hysteresis loop is more than 30 K for a crystallite size of 14 nm in VO<sub>2</sub>.
5. The study reveals that the magnetic property display opposite hysteresis shapes to any other properties (optical, electrical, roughness, surface plasmon resonance) used to study the VO<sub>2</sub> MIT so far.

---

<sup>1</sup>Author to whom correspondence is to be addressed:

Bonex Mwakikunga Email address: [bmwakikunga@csir.co.za](mailto:bmwakikunga@csir.co.za) Fax: +27 12 841 2229

**Magnetism Variations and Susceptibility Hysteresis at the Metal-Insulator Phase Transition Temperature of  $\text{VO}_2$  in a Composite Film Containing Vanadium and Tungsten Oxides**

Amos A Akande<sup>1, 2</sup>, Koena E Rammutla<sup>2</sup>, Thomas Moyo<sup>3</sup>, Nadir S E Osman<sup>3</sup>, Steven S Nkosi<sup>4</sup>, Charl Jafta<sup>5</sup>, Bonex W. Mwakikunga<sup>1,\*</sup>

<sup>1</sup>DST/CSIR National Centre for Nano-Structured Materials, P O Box 395, Pretoria 0001, South Africa

<sup>2</sup>University of Limpopo, Department of Physics, P/Bag X1106, Sovenga, 0727, RSA

<sup>3</sup>School of Chemistry and Physics, University of KwaZulu-Natal, Westville Campus, Durban, South Africa

<sup>4</sup>CSIR National Laser Centre, P O Box 395, Pretoria 0001, South Africa

<sup>5</sup>CSIR Energy and Materials, CSIR P O Box 395, Pretoria 0001, South Africa

**Abstract**

We report on the magnetic property of  $0.67\text{-WO}_3 + 0.33\text{-VO}_x$  mixture film deposit on the corning glass substrate using chemical sol gel and atmospheric pressure chemical vapour deposition (APCVD) methods. The XRD and Raman spectroscopy confirm species of both materials, and the morphological studies with FIB-SEM and TEM reveal segregation of W

---

\* Author to whom correspondence is to be addressed:

Bonex Mwakikunga Email address: [bmwakikunga@csir.co.za](mailto:bmwakikunga@csir.co.za) Fax: +27 12 841 2229

and V atoms. XPS reveals that  $V^{4+}$  from  $VO_2$  forms only 11% of the film;  $V^{3+}$  in the form of  $V_2O_3$  form 1% of the film, 21% is  $V^{5+}$  from  $V_2O_5$  and 67% is given to  $W^{6+}$  from  $WO_3$ . The analysis of the ESR data shows some sharp changes in the magnetism near the metal-to-insulator (MIT), which could be theoretically interpreted as the ordering or alignment of electron spins from net moment nature to parallel alignment of magnetic moment. The derivatives of magnetic susceptibility established the thermally induced magnetic property:- two distinct transitions of 339 K for heating data and 338 K for cooling data for 151.2 mT field were obtained. Similar results were also obtained for 308.7 mT field, 336 K for heating data and 335 K for cooling data. VSM results confirm a paramagnetic phase with a small amount of magnetically ordered phase.

**Key words:** Vanadium dioxide, Tungsten oxide, Metal-to-Insulator Transition, Paramagnetism, Magnetic susceptibility.

## 1.0 Introduction

Vanadium forms a variety of binary oxide families which are generally expressed as follows;  $V_nO_n$ ,  $V_nO_{2n}$ ,  $V_nO_{2n-1}$  and  $V_nO_{2n+1}$ , with  $VO$ ,  $V_2O_3$ ,  $VO_2$ ,  $V_6O_{13}$  and  $V_2O_5$  being part of the daughters raised by these families. These oxides have been given much attention by many researchers because of their ability to exhibit metal-insulator phase transition (MIT) as observed by Magneli, Morin, Goodenough, Adlar, Paquet, Fujimori, Peirels and Mott-Hubbard [1-11].



Among these oxides of vanadium, VO<sub>2</sub> with V<sup>4+</sup> oxidation state and 3d<sup>1</sup> configuration differs from others in its MIT properties. The MIT in VO<sub>2</sub> takes place at around 340 K, a temperature close to room temperature, and this is usually accompanied by a slight shift in its lattice structural transition from tetragonal structure (R) high temperature phase (T ≥ 340 K) to monoclinic structure (M<sub>1</sub>) low temperature phase (T < 340 K) [1],[12-13].

This structural transition has been reported to be responsible for abrupt changes in the electrical, optical and magnetic properties [14-15], although there has not been any detailed report on the magnetic property of VO<sub>2</sub> MIT. This oxide is applied in various technologies; the major being in the thermochromic applications for instance its thermally induced electrical property is employed in the sensing of gases and chemicals [16-17]. Much research has been done in the area of optoelectronics such as switchable window applications and it was reported that VO<sub>2</sub> blocks or reflects near infrared radiation in the metallic phase and allows it in the monoclinic (semi conducting/insulating) phase [18]. Other researchers have also reported the doping of tungsten metal ion into the lattice of VO<sub>2</sub> in order to enhance optical performance and possibly reduce the phase transition to room temperature [17, 19-21].

The underlying principles that explained the transitions in VO<sub>2</sub> in great detail is the electronic band structure and was described by Goodenough Model as presented in Fig. 1 that the vanadium (V<sup>4+</sup> and 3d) atom in the metallic R phase (with t<sub>2g</sub> levels in the octahedral crystal field) splits into two levels d<sub>11</sub> and π\* orbital comprising the electronic states near Fermi level of the metallic states. The d<sub>11</sub> orbital which is nonbonding together with π\* strongly hybridized with the oxygen O 2pπ\* state and consequently π\* lie in a higher level than d<sub>11</sub>. Insulating monoclinic phase is different in that the pairing of the V<sup>4+</sup> atom along Cr

axis pushes the  $3d-2p$  hybridization and up-shifts the  $\pi^*$  band away from the Fermi level and causing the bonding and anti-bonding splitting of the  $d_{11}$  which is classified as the opening of band or band gaps [1], [22].

The hysteresis thermal profile of  $\text{VO}_2$  has been studied by many scientists by measuring the structural, morphological, electronic and optical properties at varying temperatures as summarized in Fig. 2. Common results of hysteresis steps have been obtained when heating up and cooling down measurements are conducted [23-24]. Fig. 2 (a) and 2 (b) show the opposite effects or relationships with temperature for electrical resistance and conductance  $S$  and optical transmittance and reflectance, as we know from the basic definition that conductance  $S$  is inverse of resistance and similarly for reflectance and transmittance (especially when the optical absorption remain constant – Beer Lambert law). Fig. 2 (c) and 2 (d) speaks of the surface effect near the MIT while Fig. 2 (e) is the Raman study of the phonon frequency and Fig. 2(f) the effect of surface plasmon resonance wavelength near MIT.

The electronic (resistance and or conductance) property of  $\text{VO}_2$  was explained by Goodenough as illustrated above Fig. 1, the electrostatic consideration for the effective ionic charges (electron to electron interaction) using anti-ferro-electric as potential driving force for the MIT.

From this explanation, a number of experiments have been conducted [21-22] [24] and it was found that the reason for MIT in  $\text{VO}_2$  may be due to the electron to electron interaction between the two ions of vanadium and oxygen. Optical studies of  $\text{VO}_2$  property (transmittance and or reflectance) [21-24] also explained the switching from monoclinic structure (insulating) to tetragonal (metallic) structure as a function of temperature.

The transition in VO<sub>2</sub> is thought to occur due to the effect of lattice distortion (lattice atomic arrangement) and electronic band structure; it follows that **the low-temperature monoclinic (insulating) phase may exhibit high refractive index, and thus allow huge amount of near-infrared radiation while high-temperature tetragonal (metallic) phase may have low refractive index and thereby blocking this radiation [25-26].**

Recently Lopez et al [12] [27] and Lysenko et al [28] also presented the thermal hysteresis profile study of VO<sub>2</sub> using the Fig. 2 (c) surface roughness (nm) and Fig. 2 (d) scattering (arbitrary unit) of time-resolved light and X-ray diffraction. The MIT in VO<sub>2</sub> is said to be related to the nucleation mechanism of VO<sub>2</sub> crystal [27] and the hysteresis profile of the scattering intensity shows unique changes revealing non-linear absorption characteristic in VO<sub>2</sub> [28].

Phonon studies from **Raman spectra have been used to explain the MIT transition of VO<sub>2</sub> and were done by comparing the modes (vibrational, rotational, or stretching)** of the room temperature ambient pressure Raman spectrum with the spectrum at transition temperature [29-32]. In these studies, the 617 cm<sup>-1</sup> phonon known as the characteristic wavenumber (although with slight variation depending on the particle size) produced reduced relative intensity near the MIT [23]. This method has shown some convincing thermal hysteresis profile of VO<sub>2</sub> from various experiments as the results show emergence of shifting in phonon frequency or relative intensity from low temperature monoclinic (insulator) phase to high temperature tetragonal (metallic) phase [23-24].

Also recently Maaza *et. al.* [33] presented the thermally induced tunability of surface plasmon resonance property of VO<sub>2</sub> with the aim of producing VO<sub>2</sub> nano-photonics device. The electron resonance effect occurs when the frequency of the photon matches the

natural frequency of the surface electrons in the material, for VO<sub>2</sub>, huge shift in surface plasmon resonance wavelength was observed in Fig. 2 (f) from insulating state to metallic state.

In the present work, we begin by confirming the MIT of the present VO<sub>2</sub> containing samples by the traditional method of monitoring its conductivity as function of temperature. Once confirmed that the MIT at 340 K is present then we move to new properties – **magnetism changes** around the VO<sub>2</sub> MIT and **sharp changes in the** magnetic susceptibility.

VO<sub>2</sub> is known to be a paramagnetic material with unpaired electrons, which have electronic structure that leaves electron in a state in such a way that it does not have a partner of opposite spin. Most transition metals have this magnetic behaviour as they possess surface free standing clusters or centres and this has become **of** great interest as there is a possibility for ferromagnetism in low-dimensional paramagnetic materials [34].

Imada et al [1] **and reference therein presented** the first magnetic studies of VO<sub>2</sub> theoretically and experimentally by using NMR and EPR, it was discovered that the M<sub>1</sub> phase (ground state) is nonmagnetic with the vanadium atoms both paired and twisted from the rutile position. They observed the emergence of other phases, namely, monoclinic, M<sub>2</sub> and triclinic, T, at higher temperature before reaching the transition temperature, these phases show some magnetic charge ordering as  $S = \frac{1}{2}$  Heisenberg chains. The M<sub>2</sub> transition is seen as Mott-Hubbard insulator while T is regarded as the spin Peierls insulator although the transition between M<sub>2</sub> and T is a weak first order transition [1, 11].

Akoh et al. [35] also have proved experimentally that the vanadium atom which is paramagnetic shows some existence of magnetism. They further stressed that the isolated

or structured atom of vanadium have a permanent magnetic moment of  $3 \mu_B$ , whereas, the bulk vanadium atom does not exhibit any magnetic property. The magnetic property of overlaid systems of vanadium atom with tungsten has also been considered and the results show the enhancement of magnetic property of vanadium by the hybridization of V and W d-bands [36].

## **2.0 Theoretical considerations**

### **2.1 Mott theory of MIT in insulating or polycrystalline material**

N.F Mott in 1968 proposed a model for DC electrical conductivity in multi-phase or disordered systems such as amorphous materials, compounds and alloys and polycrystalline semiconductor systems at varying temperatures [40]. In his theory, electrical conduction is considered in terms phonon assisted or phonon-mediated hopping of electrons from one localized state (cat-ionic state or site) to another within the band gaps of disorder systems.

The electron hopping occurs between states of low thermal energy to states of higher energy, Mott pointed out that the charge transport could also be as a result of the tunnelling process whereby the electron hops from one state to another that has equal energy or from a higher energy to a state of lower energy with the release or emission of phonons.

The term Variable Range Hopping (VRH) is explained in the light of the characteristic hopping length and thermal activation energy between cationic states or sites. Mott's model thus generally states that the electron conductivity is given as:

$$\sigma(T) = \frac{\nu_0 N q^2 R^2}{k_B T} \alpha(1-\alpha) \exp(-2\beta R) \exp[-W/k_B T] \quad (5)$$

where  $\nu_0$  is the longitudinal optical (LO) phonon frequency,  $N$  is the total number of sites of transition metal cat-ions per unit volume,  $q$  is the electronic charge,  $R$  is the average separation between transition metal cat-ions,  $\alpha$  is the fraction between the number of cat-ions in the high valence state and low valence state,  $\beta$  is the attenuation factor which is the inverse localization length of the radial wave function,  $W$  is the activation energy and  $k_B$ , the Boltzmann constant.

Mott's equation is linearized herein in the following manner:

$$\ln(\sigma.T) = \ln \left[ \frac{\nu_0 N q^2 R^2}{k_B} \alpha(1-\alpha) \right] - 2\beta R - \frac{W}{k_B T} \quad (6)$$

The solution suggests that a plot of  $\ln(\sigma.T)$  against  $1/T$ , will yield a linear graph whose slope equals to  $-W/k_B$  and the intercept  $\ln[\alpha(1-\alpha)\{(\nu_0 N q^2 R^2)/k_B T\}] - 2\beta R$ . From the slope one can calculate the activation energy  $W$  and the intercept, the values of  $R$  can be determined from known values of  $\alpha$  and  $\beta$ .

## 2.2 Magnetic moment, magnetization and magnetic susceptibility

In this section, the authors considered it necessary to briefly refresh the definition and interrelations among some of the magnetic quantities, such as magnetic moment, magnetization and magnetic susceptibility that are needed in this report. These quantities could be explained by using the Curie-Weiss law [ $\chi = C/(T-T_c)$ ] where  $C$  is a constant and  $T_c$  is the Curie temperature. This law has been used for various studies of temperature

dependent magnetic susceptibility. At  $T \gg T_c$ , the law is modified to  $\chi = C/(T-T_c)^\gamma$  where  $\gamma$  is an constant exponent. The effect of an external magnetic field  $H_0$  on a particle with spin  $S$ , is to force the spin magnetic moment  $\mu$  to precess (or re-orient or align) along  $H_0$ , that is to split the energy of the  $S$  manifold [36].

In many body systems, this can results in the population of different levels according to Boltzmann law, and thus the number of particles in the lower energy state with magnetic moment aligned with the field is higher than those in higher energy state with magnetic moment opposite to the field. As a result, the induced magnetic field along  $H_0$  is possible and the magnetization per unit volume  $M$  corresponds to the induced magnetic moment per unit volume. For a numbers of materials, the induced magnetic moment is proportional to the applied magnetic field  $H_0$  [36-37]. All this quantities could be expressed as [38]

$$M = \frac{\mu_{induced}}{V} = \chi_{volume} H_0 \quad (1)$$

where  $\mu_{induced}$  is the magnetic moment density and  $\chi_{volume}$  is the dimensionless proportionality constant between  $M$  and  $H_0$  which is known as the magnetic susceptibility per unit volume of the material. Magnetic quantities could also be obtained from the Helmholtz thermodynamic free energy relation for magnetic systems [39]

$$F = U - TS - M \bullet H \quad (2)$$

where  $U$  is the internal energy of the electron spins,  $S$  is entropy of the system and  $T$  is the temperature. From this, the first derivative of function  $F$  with respect to  $T$  could give the measure of the spins disorder in the system (entropy) [37-38]. Our major interest in

[Equation (2)] is the quantity  $M.H$  which represents magnetic energy, the negative of the first derivative of the function will give magnetisation  $M$  as expressed as [39]

$$-\frac{\partial F}{\partial H} = M \quad (3)$$

Taking the derivative of [Equation (3)] with respect to  $H$ , we have the magnetic susceptibility [39]

$$\frac{-\partial^2 F}{\partial^2 H} = \chi \quad (4)$$

From the previous experimental reports, thermodynamic quantities are known to grow rapidly in the vicinity of phase transition or have a step-wise change at  $T_c$ . This transition could be first, second or third order derivatives of the free energy function and the paramagnetic to ferromagnetic phase transition are a second order of magnetic susceptibility [38-39].

### 2.3 Electron Spin Resonance Techniques

Electron spin resonance (ESR) is a spectroscopic technique that depends upon the property that any atomic system with unpaired electrons possesses a net magnetic moment which will interact with the external magnetic field. For the case of free atom containing a single unpaired electron, the electron has one of the two possible spin directions, corresponding to the allowed values of the spin quantum numbers ( $S = -\frac{1}{2}$  or  $+\frac{1}{2}$ ). The energies of the two spin states are equal in the absence of magnetic field while their energies reduced and increase respectively by  $\frac{1}{2}(g\beta H)$  as the magnetic field is applied where  $\beta = e\hbar/2mc$  called



Bohr magnetron and  $g$  is the spectroscopic Zeeman splitting factor with a value of 2.0023 for a free electron [38].

### 3.0 Experimental

The study's initial material consists of ammonium meta-vanadate [ $\text{NH}_4\text{VO}_3 \cdot 6\text{H}_2\text{O}$ ] and ammonium meta-tungstate [ $(\text{NH}_4)_6\text{W}_7\text{O}_{24} \cdot 6\text{H}_2\text{O}$ ] which were in hydrate form. The [ $\text{NH}_4\text{VO}_3 \cdot 6\text{H}_2\text{O}$ ] is a whitish powder with molecular weight of 116.98 a.m.u and density of  $2.3 \text{ g cm}^{-3}$ , its melting temperature is  $200^\circ\text{C}$  while [ $(\text{NH}_4)_6\text{W}_7\text{O}_{24} \cdot 6\text{H}_2\text{O}$ ] is a white trace metal basis powder of molecular weight 2972.0 a.m.u, solubility of  $0.1 \text{ g mol}^{-1}$  and melting temperature of  $700^\circ\text{C}$ .

These materials were dissolved gently in equal ratio in distilled water using magnetic stirring method with heater temperature raised to about  $70^\circ\text{C}$  for 15 hours to make our precursor. The substrate (corning glass) was cleaned several times by suspending them into glass test tube containing distilled water and agitated in ultrasonic wave water bath for about 10 minutes each times and at  $30^\circ\text{C}$ . The traditional sol gel dip coating technique was employed to ensure that the gel-precursor sticks to the glass substrate; this substrate was then dipped into the precursor and exposed to the atmosphere at room temperature for 72 hours. The outcome was thick film deposits, and annealing was performed at  $700^\circ\text{C}$  in APCVD reactor under the influence of  $15 \text{ L min}^{-1}$  hydrogen gas for 2 hrs.

The X-Ray diffraction scans were carried out using Panalytical X'pert Pro PW 3040/60 X-Ray diffractometer equipped with  $\text{Cu K}\alpha$  ( $\lambda=0.154 \text{ nm}$ ) monochromatic radiation source. The

measurements were extracted at 45.0 kV and 40.0 mA, and the experimental procedure shows a good reproducibility of results.

Topographical study and elemental composition were carried out using JOEL 2100 Transmission electron microscopy (TEM) (from Tokyo Japan) equipped with LaB6 filament and a Gatan U1000 camera with  $2028 \times 2028$  pixels, with high quality inbuilt Energy dispersive X-ray spectroscopy, this was used to study the lamellar layer of the VO<sub>2</sub> thin film mixed with tungsten and deposited on copper grid prepared using focussed ion beam scanning electron microscopy (FIB-SEM).

The electrical measurements were performed using the KEITHLEY 4200 Semiconductor Characterization Systems (SCS) with a collinear four point probe system and four supply-and-measure unit (SMU), all from Cascade Microtech, Inc., Oregon U.S.A. The film average resistance for -30 V to +30 V voltage sweeps from below room to above transition temperature (heating cycle) were measured using IKA® RCT basic laboratory heater. The cooling cycle forms of these measurements were also considered.

Raman spectroscopy was conducted using a Jobin–Yvon T64000 Raman spectrograph with a 514.5 nm line from an argon ion laser. The power of the laser at the sample was small enough (0.384 mW) in order to minimise localised heating of the sample. The T64000 was operated in single spectrograph mode, with the 1800 lines/mm grating and a 100× objective on the microscope.

The magnetic characterization was conducted using JOEL (JES-FA 200) ESR Spectrometer equipped with X-band (8-12 GHz) microwave and liquid helium variable temperature systems. The sample was prepared by targeting the vanadium atom deposit spot in the film

and cutting a 0.5 mm diameter fraction and the scanning were performed from room to above VO<sub>2</sub> transition temperature (291 K – 420 K) for heating and cooling cycles measurement.

#### 4.0 Results and Discussion

Fig. 3 (a) shows the X-ray diffraction pattern of the product of the materials described in the experimental section, this reveals some prominent peaks of VO<sub>2</sub> monoclinic phase with (011) orientation, (010) of V<sub>2</sub>O<sub>5</sub> and metastable phase VO<sub>2</sub> (B) in (003) orientation. VO<sub>2</sub> (B) metastable was found to have a good performance in lithium batteries [13] [41-42]. These orientations were determined from the Institute for Crystallographic and Diffraction Database– [PDF # 44-0252 (for VO<sub>2</sub> M<sub>1</sub>), 89-0611 (for V<sub>2</sub>O<sub>5</sub>) and Refs. 13, 51,52 for VO<sub>2</sub> (B)]. The profile also shows some metallic phase of W with (110) (200) and (211) orientations and WO<sub>3</sub> (200) resulting from (NH<sub>4</sub>)<sub>6</sub>W<sub>7</sub>O<sub>24</sub>.6H<sub>2</sub>O). This has been reported in [43] that around 700<sup>o</sup>C, (NH<sub>4</sub>)<sub>6</sub>W<sub>7</sub>O<sub>24</sub>.6H<sub>2</sub>O) produced metallic tungsten and WO<sub>3</sub> phases. The particle size of the VO<sub>2</sub> (M<sub>1</sub>) (011) was found to be 21 nm using Williamson and Hull techniques with 0.208<sup>o</sup> FWHM and the mean crystallite diameter of 40 nm for the entire profile was obtained. Raman spectrum (RS) of the system is presented in Fig. 3 (b) and it produced similar results with the X-ray diffraction pattern in Fig. 3 (a).

RS is known to be good for surface analysis of material. The 146 cm<sup>-1</sup> band has been attributed to the chain translation mode of V<sub>2</sub>O<sub>5</sub> reduction to VO<sub>2</sub>, with NH<sub>4</sub>VO<sub>3</sub>. 6H<sub>2</sub>O as a precursor [44]. Bands of 142 cm<sup>-1</sup> and 258 cm<sup>-1</sup> were also reported as VO<sub>2</sub> monoclinic phase [45] and are in a close range to the bands observed in the spectrum. However, tungsten

peaks were found to dominate in the spectrum,  $77\text{ cm}^{-1}$ ,  $684\text{ cm}^{-1}$  and  $804\text{ cm}^{-1}$  are the characteristic bands of  $\text{WO}_3$  for monoclinic, N, and triclinic phase respectively [46] while  $978\text{ cm}^{-1}$  also close to the  $\text{V}=\text{O}$  band of  $\text{V}_2\text{O}_5$  vibration.

XPS data are presented in Fig 3 (c). This figure shows that the film is composed of W, O and V in various states. Higher resolution of W area reveals two Gaussian peak which are assigned to  $\text{W}^{6+}$  ( $4f_{7/2}$ ) and  $\text{W}^{6+}$  ( $4f_{5/2}$ ). This means that W is in one major electronic state W 4f which may signify presence of  $\text{WO}_3$  and this is confirmed by Raman spectroscopy by the peak at  $800\text{ cm}^{-1}$  in Fig 3 (b). Higher resolution of the V area in the XPS data of Fig 3 (c) but now given Fig 3 (e) shows a peak which asymmetric revealing that there are several state of the V ion. De-convolution of the peak indicated that there two major phases:  $\text{V}^{4+}$  and  $\text{V}^{5+}$ . There is a trace amount of the  $\text{V}^{3+}$  electronic state in this peak but it was found to be negligible.

Comparison of W and V areas show that 67% of the film is  $\text{WO}_3$  while 33% is  $\text{VO}_x$  of various ionic states. Further comparison of the V peak de-convolution shows that  $\text{V}^{4+}$  from  $\text{VO}_2$  forms only 11% of the film;  $\text{V}^{3+}$  in the form of  $\text{V}_2\text{O}_3$  form 1% of the film, 21% is  $\text{V}^{5+}$  from  $\text{V}_2\text{O}_5$  and 67% is given to  $\text{W}^{6+}$  from  $\text{WO}_3$ . XPS should not further distinguish between the polymorphs of  $\text{VO}_2$  such as  $\text{VO}_2$  M1,  $\text{VO}_2$  (B) or  $\text{VO}_2$  (A) as they are all in the  $\text{V}^{4+}$  ionic state of vanadium.

The SEM image in Fig. 4 (a) shows the existence of segregation of atoms in the mixed  $\text{VO}_2$   $|\text{V}_2\text{O}_5|$  $\text{WO}_3$  system as opposed to the expected diffusion of W and V atoms. This may be due to the effect of high concentration of W-atom in  $\text{VO}_2$  lattice and also the fact that W atom has high atomic weight compared to V atom. Optical performance of high concentration Ti and W cations has been previously reported [47-48]. The elemental

quantity picture was presented in Fig. 4 (b), W, V and oxygen atoms were present at the surface while Na, Ca and K are the elements from the glass substrate. Fig. 4 (c) represents the TEM study of the heavily W-alloyed VO<sub>2</sub> deposit on the lamellar copper grid from FIB-SEM set-up. Scanning sweeps were performed at several spots of the copper grid, the image shows V localized sites on the silicon substrate (corning glass) with Fig. 4 (d) the corresponding elemental profile showing the segregation of V atom from W. Fig. 4 (e) shows hybridization of W and V atom with Fig. 4 (f) showing the corresponding elements profile and the selected area electronic diffraction pattern.

The current-voltage characteristics curves of the VO<sub>2</sub> spot in film are presented in Fig. 5, the curves in Fig. 5 (a) were for heating cycle from 24 °C to 80 °C and Fig. 5 (b) were for cooling cycle from 80 °C back to 24 °C. These measurements show some shifts in the resistance of the material as we change temperature from low to high which confirm the thermally induced MIT nature of VO<sub>2</sub> and this shows that Vanadium atoms override tungsten atoms in forming metal oxide due to their high energy of formation of -7.03 eV/mol compared to 8.42 eV/mol for W [49].

The average resistance for each measurement were plotted against the temperatures and the resulting picture is the hysteresis loop in Fig. 5 (c) with two distinct steps, the first at high resistant insulating (monoclinic) phase and the other at low resistant metallic (metallic) phase. Fig. 5 (d), the plot of Mott's model that was discussed in section 2.2 of this report shows similar steps trend for the product of conductivity and temperature versus the inverse of temperature. Both heating and cooling cycle's data were fitted linearly to obtain the activation energy of hopping electrons in the material as {Eq. (6)} suggested. It was

found that the energies are 0.066 eV for heating and 0.054 eV for cooling. The heating hopping value of 0.128 eV has been reported for VO<sub>2</sub> nanowire [50].

Magnetic property of the spot was investigated and Fig. 6 shows the ESR spectrum in Fig. 6 (a) for heating measurements from 291 K to 420 K, and 7 (b) for cooling measurements from 303 K to 403 K. Two distinct sharp peaks of materials were observed, one at a low field of 151.2 mT and the other at a high field of 308.7 mT. These spectra show some improvement in intensity of the material as the temperature changes which indicates the ordering/alignment of the electron spins in the material with respect to increase in temperature and consequently the increase in magnetic moment.

Some authors on ESR have ascribed sharp ESR line-shapes to para-magnetism and broad ESR line-shapes to ferro-magnetism [53]. This argument is based on the fact that ESR is in fact sometimes referred to as EPR (electron paramagnetic resonance) and therefore sharp and intense resonances are ascribed to para-magnetism. However other authors [54] on ESR have explained sharp or broad as ferro or para respectively to the contrary; this difference in opinions shows that the use of the nature of the ESR line-shapes to ferro or para magnetism is not yet resolved in ESR or EPR. In order to ascertain the para or ferro magnetism in this film, we have undertaken Vibrating Sample Magnetometry (VSM) in order to obtain M vs H hysteresis curves. We have obtained M vs H hysteresis curves from a commercial and pure VO<sub>2</sub> samples.

Fig. 6 (c) displays the plot of magnetization, M, against the applied field, H, from the VSM technique. This plot reveals that the film is composed of a paramagnetic phase and a small ordered phase. The shift of the hysteresis loop away from the (0,0) point is a clear indication of the multi-phase nature of the film which may present frozen magnetic moments of

varying orientations such that it takes a finite threshold applied field in order to bring all these moments to a net zero magnetization. Above such a threshold ( $H_T$ ) field, the moments align with the applied field and a finite amount of magnetization appears in the sample. The shift in the M-H plots in Fig 6 (c-e) may be attributed to “exchange bias effect”[55] which is observed in nano-scale materials.

The plots of the inverse of intensity versus temperature were presented in Fig. 7. In Fig. 7 (a) 151.2 mT peaks was considered for both heating and cooling measurements with an agreement around 338 K, and in Fig. 7 (b) 308.7 mT peaks was considered for both heating and cooling measurements and also with an agreement around 336 K. Fig. 7 (c and d) shows the derivative magnetic susceptibility of the ESR data that was calculated using {Equation (1)} and the derivative of the results was considered for phase transition as explained in section 2.2 of this report. Fig. 7 (c) shows the derivative magnetic susceptibility for heating and cooling data produced by 151.2 mT field and Fig 7 (d) presents the derivative magnetic susceptibility for heating and cooling data produced by 308.7 mT. Two distinct transitions of 339 K for heating and 338 K for cooling data for 151.2 mT field were obtained and similar results were also obtained for 308.7 mT field i.e. 336 K for heating and 335 K for cooling data, respectively.

Hysteresis width in the changes of the magnetic and susceptibility MIT is found to be 1K. When compared to the hysteresis in the electrical conductivity MIT in Fig. 5 (c) of more than 30 K, one leads to the fact that magnetic properties, though linked to electronic properties, display completely different hysteresis characteristics. The hysteresis loop width in most of the properties reviewed above: conductivity, optical, phonon intensity, surface roughness

and surface plasmon resonance all display a widening hysteresis loop as the crystallite size decreases.

## 5.0 Conclusion

In summary we have reported the magnetic property of heavily **W-alloyed** VO<sub>2</sub> system; the ESR method has proven that VO<sub>2</sub> **has a huge change in magnetic properties around its MIT**. Transition was found to occur around the MIT, 339 K for heating data and 338 K for cooling data for 151.2 *mT* field peaks and similarly 336 K for heating data and 335 K for cooling data 308.7 *mT* field peaks. This MIT was confirmed with electrical measurement and the result shows a shift in the resistance of the material from the insulating state to the metallic state. Segregation of W and V atoms is observed as opposed to their diffusion. This could be due to the high concentration of W. Finally, there is a hybridization of O 2*p* in favour of vanadium atoms rather than tungsten atoms due to the high energy of formation of the vanadium dioxide. Magnetic susceptibility as a function of temperature is presented here as another means of tracking the VO<sub>2</sub> metal-to-insulator transition temperature.

## Acknowledgements

The authors acknowledge the financial support from the India-Brazil-South Africa trilateral programme with a project number HGER24X and the CSIR National Centre for Nano-Structured Materials project number HGER27S.



## References

- [1] M. Imada, A. Fujimori, Y. Tokura, Metal-insulator transitions, Rev. of Modern Phy 70, No. 4 1039-1263 (1998).
- [2] N.F. Mott, Metal-insulator Transition, Rev. Modern Phys. 40 (4) (1968) 677.
- [3] D. Adler, Mechanisms for Metal-Nonmetal Transitions in Transitions-Metal Oxides and Sulfides, Rev. Modern Phys. 40 (4) (1968) 714-736.
- [4] F.J. Morin, Oxides which show a metal-insulator-transition at Neel temperature, Phys. Rev. Lett. 3, (1959) 34.
- [5] P. Kiria, G. Hyettb, R. Binions, Solid state thermochromic materials, Adv. Mat. Lett. 1(2), 86-105 (2010)
- [6] J.B. Goodenough, The two components of Crystallographic transition in VO<sub>2</sub>, J. Solid State Chem. 3, 490-500 (1971).
- [7] S. Shin, S. Suga, M. Tanuguchi, M. Fijisawa, H. Kanski, A. Fujimori, H. Damon, Y. Ueda, K. Kosuge, S. Kachi, Vacuum-ultraviolet reflectance and photoemission study of the metal-insulator phase transitions in VO<sub>2</sub>, V<sub>6</sub>O<sub>13</sub>, and V<sub>2</sub>O<sub>3</sub>, Phys. Rev. B 41, 4993-5009 (1990).
- [8] J.M. Reyes, J.R. Marko and M.Sayer, Hysteresis in the Semiconductor-Metal Transition of Cr-doped VO<sub>2</sub>, Sol. St. Comm, Vol. 13 1953-1957 (1973)
- [9] D. Paquet, P. Leroux-Hugon, Electron correlations and electron-lattice interactions in the metal-insulator, ferroelastic transition in VO<sub>2</sub>: A thermodynamical study, Phys. Rev. B22, 5284-5301 (1980).
- [10] N.F. Mott, R. Peierls, Discussion of the paper by de Boer and Verwey Proc. Phys. Soc. London, Ser. A. 49, 72 (1937).

- [11] A. I. Buzdin, L. N. Bulaevskii, P. N. Lebedev, Spin-Peierls transition in quasi-one-dimensional crystals, Physics Institute, Academy of Sciences of the USSR, Moscow Usp Fiz Nauk, 131, 495-510 (July 1980).
- [12] R. Lopez, L.A. Boatner, T.E. Haynes, R.F. Haglund, Jr. Feldman, L.C. Feldman, Enhanced hysteresis in the semiconductor-to-metal phase transition of VO<sub>2</sub> precipitates formed in SiO<sub>2</sub> by ion implantation, Phy Letters 79 (2001) 19.
- [13] X.J. Wang, H.D. Li, Y.J. Fei, X. Wang, Y.Y. Xiong, Y.X. Nei, K.A. Feng, XRD and Raman study of vanadium oxide thin film deposits on fused silica substrates by RF Magnetron Sputtering, Applied surface science 177 (2001) 8-14.
- [14] M-H. Lee, J.S. Cho, Better Thermochromic glazing of windows with ant-reflection coating, Thin Solid Film 365 5-6 (2000).
- [15] L. Alberto, L. de Almeida, G. S. Deep, A. Mercus, N. Lima, H. Neff and R. S. Freire, A Hysteresis Model for Vanadium Oxide Thermal Radiation Sensor, IEEE Instrumentation Measurement Technology Conference 2000.
- [16] E. Strelcov, Y. Lilach, A. Kolmakov, Gas Sensor Based on Metal-Insulator Transition in VO<sub>2</sub> Nanowire Thermistor, Nano Letters 2009, Vol. 9, No. 6, 2322-2326
- [17] A. Pergrament, G. Stefanovich, O. Berezina, D. Kirienko, Electrical conductivity of tungsten doped vanadium dioxide obtained by the sol-gel technique, Thin Solid Films 572-576 (2013)
- [18] Y. Gao, H. Luo, Z. Zhang, L. Kang, Z. Chen, J. Du, M. Kanehira, C. Cao, Nanoceramic VO<sub>2</sub> thermochromic smart glass: A review on progress in solution processing, Nano Energy (2012) 1, 221-246.

- [19] W. Burkhardt, T. Christmann, B.K. Meyer, W. Niessner, D. Schalch, A. Scharmann, W- and F-doped VO<sub>2</sub> films studied by photoelectron spectrometry, *Thin Sol. Films.* 345 (1999) 229-235.
- [20] O. Y. Berezina, A. A. Velichko, L.A. Lugovskaya, A.L. Pergament, G.B. Stefanovich, D.V. Artyukhin, A. N. Strelko, Properties of Tungsten-Doped Vanadium Oxide Films, *Tech. Phys. Lett.* (2007) Vol. 33, No. 7, pp. 552-555.
- [21] R. Binions, G. Hyett, C. Piccirillo, I. P. Parkin, Doped and Undoped vanadium dioxide thin films prepared by atmospheric pressure chemical vapour deposition from vanadyl acetylacetonate and tungsten hexachloride: the effects of thickness and crystallographic orientation on thermochromic properties, *J. Mat. Chem.* 17, 4652-4660 (2007)
- [22] V. Eyert, The metal-insulator transitions of VO<sub>2</sub>: A band theoretical approach *Ann. Phys. (Leipzig)* 11, 1-61 (2002) 9.
- [23] M. Pan, J. Liu, H-M. Zhong, S-W. Wang, Z-F. Li, X-S. Chen, Wei Lu, Raman study of the phase transition in VO<sub>2</sub> thin films *J. of Cry. Growth* 268 (2004) 178-183
- [24] C. Marini, E. Arcangeletti, D. Di Castro, L. Baldassare, A. Perucchi, S. Lupi, L. Malavasi, L. Boeri, E. Pomjakushina, K. Conder, P. Postorino, Optical properties of V<sub>1-x</sub>Cr<sub>x</sub>O<sub>2</sub> compounds under high pressure, *Phy Rev. B* 77, 235111-9, 2008
- [25] B. W. Mwakikunga, E. Sideras-Haddad, M. Maaza, First synthesis of vanadium dioxide by ultrasonic nebula-spray pyrolysis, *Optical Materials* 29 (2007) 481-487
- [26] S.-Y. Li, G. A. Niklasson, and C. G. Granqvist, Nanothermochromics: Calculations for VO<sub>2</sub> nanoparticles in dielectric hosts show much improved luminous transmittance and solar energy transmittance modulation, *J. Appl. Phys.* 108, 063525 (2010).

- [27] R. Lopez, R. F. Haglund, Jr., L. C. Feldman, L. A. Boatner, T. E. Hayness, Optical nonlinearities in VO<sub>2</sub> nanoparticles and thin films, *App. Phys. Lett.* 85, (2004).
- [28] S. Lysenko, A. Rua, F. Fernandez, H. Liu, Vanadium dioxide based plasmonic modulators, *J. Appl. Phys.* 105, 043502 (2009)
- [29] J. Cao, W. Fan, J-Q. Wu, Strain and temperature dependence of the insulating phases of VO<sub>2</sub> near the metal-insulator transition, *Phy. Rev. B* 85, 020101(R) (2012)
- [30] Z. Lu, C-G.Lia, Y. Yin, Synthesis and thermochromic properties of vanadium dioxide colloidal Particles, *J. Mater. Chem.*, 2011, 21, 14776-14782
- [31] E .U. Donev, J. I. Ziegler, R. F Haglund Jr., L. C. Feldman, Size effects in the structural phase transition of VO<sub>2</sub> nanoparticles studied by surface-enhanced Raman scattering, *J. Opt. A: Pure Appl. Opt.* 11(2009) 125002 (8pp).
- [32] A. C. Jones, S. Berweger, J. Wei, D. Cobden, M. B. Raschke, Nano-optical investigations of the metal-insulator phase behaviour of individual VO(2) microcrystals, *Nano Lett.* 2010, 10, 1574–1581.
- [33] M. Maaza, O. Nemraoui, C. Sella, A. C. Beye, B. Baruch-Barak, Thermal induced tenability of surface plasmon resonance in Au-VO<sub>2</sub> nano-photonics, *Optics Comm.* 254 (2005) 188-195.
- [34] J. Khalifeh, Magnetic structure of vanadium overlayers on semi-infinite substrate, *J. Mag. Mat.* 168 (1997) 25-30.
- [35] H. Akoh and A. Tasaki, Appearance of Magnetic moments in Hyperfine particles of Vanadium Metal, *J. Phys. Soc. Jap.* 42, 791 (1977).

- [36] A. M. Bakir, B. A. Hamad, J. M. Khalifeh, Surface and interface magnetism of V/W systems, *phys. stat. sol. (b)* 242, No. 12, 2522–2529 (2005)
- [37] I. Bertini, C. Luchinat, G. Patirigi, Magnetic susceptibility in paramagnetic NMR, *Prog. in N.M.R. Spec.* 40 (2002) 247-273.
- [38] R. Boca, Mean and differential magnetic susceptibilities in metal complexes, *Coord Chem. Rev.* 173 (1998) 167–283.
- [39] M. D. Vannette, Dynamic magnetic susceptibility of systems with long-range magnetic order, Graduate Theses and Dissertations, Iowa State University, <http://lib.dr.iastate.edu/etd> (2009).
- [40] N.F. Mott, Conduction in glasses containing transition metal ions, *J. Non-Cryst. Solids* 1 (1968) 1-17
- [41] S. A. Corr, M. Grossman, Y. Shi, K. R. Heier, G. D. Stucky, R. Seshadri, VO<sub>2</sub>(B) nanorods: solvothermal preparation, electrical properties, and conversion to rutile VO<sub>2</sub> and V<sub>2</sub>O<sub>3</sub>, *Mater. Chem.*, 2009, 19, 4362–4367
- [42] S. Pavasupree, Y. Suzuki, A. Kitiyanan, S. Pivsa-Art, S. Yoshikawa, Synthesis and Characterization of vanadium oxides nanorods, *J. Solid State Chem.* 178 (2005) 2152–2158
- [43] B.W. Mwakikunga, E. Sideras-Haddad, C. Arendse, M. J. Witcomb, A. Forbes, Raman spectroscopy of WO<sub>3</sub> nano-wires and thermo-chromism study of VO<sub>2</sub> belts produced by ultrasonic spray and laser pyrolysis techniques, *J. Nanosc. & Nanotech.* Vol. 8, 1-9, 2008
- [44] C. Julien, G. A. Nazri, and O. Bergstrom, Raman Scattering Studies of Microcrystalline V<sub>6</sub>O<sub>13</sub>, *Phys. Stat. Solidi B* 201, 319-326 (1997)

- [45] G.I. Petrov, V.V. Yakovlev, J. Squier, Raman microscopy analysis of phase transformation mechanisms in vanadium dioxide Appl. Phys. Lett. 81 (6) (2002) 1023-1025.
- [46] E. Cazzanelli, C. Vinegoni, G. Mariotto, A. Kuzmin, and J. Puransà, Low-Temperature Polymorphism in Tungsten Trioxide Powders and Its Dependence on Mechanical Treatments, J. of Sol. St. Chem. 143, 24-32 (1999).
- [47] F. Beteille, J. Livage, Optical Switching in VO<sub>2</sub> Thin films, J. of Sol-Gel Sc. and Tech. 13, 915–921 (1998)
- [48] C. S. Blackman, C. Piccirillo, R. Binions, Ivan P. Parkin, Atmospheric pressure chemical vapour deposition of thermochromic tungsten doped vanadium dioxide thin films for use in architectural glazing, Thin Solid Films 517 (2009) 4565–4570.
- [49] B W Mwakikunga, A. E. Mudau, N. Brink, C.J. Willers, Flame temperature trends in reacting vanadium and tungsten ethoxide fluid sprays during CO<sub>2</sub>-laser pyrolysis, Appl. Phys B 105, 451-462 (2011).
- [50] X. Wu, Y. Tao, L. Dong, Z. Wang, Z. Hu, Preparation of VO<sub>2</sub> nanowires and their electric characterization, Mat. Res. Bullet. 40 (2005) 315–321.
- [51] F. Theobald, R. Cabala, J. Bernard, Test on the structure of VO<sub>2</sub> (B), J. Solid State Chem., 17 (1976) 431
- [52] Y. Oka, T. Yao, N. Yamamoto, Y. Ueda, A. Hayashi, Phase transition and V<sup>4+</sup>-V<sup>4+</sup> pairing in VO<sub>2</sub> (B), J. Solid State Chem. 105 (1993) 271
- [53] S. S. Nkosi, H. M. Gavi, D. E. Motaung, J. Keartland, E. Sideras-Haddad, A. Forbes, B. W. Mwakikunga, Ferromagnetic resonance characterization of nano-FePt by electron spin resonance, J. Spectrosc. 2013 (2013) art ID 272704, 6 pages

[54] A. Martins, S. C. Trippe, A. D. Santos, F. Pelegrini, Spin-wave resonance and magnetic anisotropy in FePt thin films, *J. Magnetism Magnetic Mater.* 302 (2007) 120-125

[55] J Nogués, J Sort, V. Langlais, V. Skumryev, S. Surinack, J. S. Muñoz, M. D. Baró, Exchange bias in nanostructures, *Phys. Rep.* 422 (2005) 65-117

## Figure Captions

Fig. 1 The electronic energy band diagram of the VO<sub>2</sub> system as proposed by Goodenough [6].

Fig. 2 Variation of VO<sub>2</sub> properties with temperature close to MIT: (a) Resistance and Conductance, (b) Transmittance and Reflectance, (c) Roughness (d) Scattering, (e) Raman relative intensity of 618 cm<sup>-1</sup> phonon frequency and (f) Surface Plasmon resonance wavelength.

Fig. 3 (a) X-Ray diffraction pattern of the mixtures of WO<sub>3</sub> and VO<sub>x</sub> film (b) Room temperature Raman spectrum of the same film (c) XPS spectrum of the film (d) Higher resolution XPS of the WO<sub>x</sub> regions (e) Higher resolution XPS of the VO<sub>x</sub> regions.

Fig. 4 (a) SEM mapping of VO<sub>2</sub> and W over layered system, (b) corresponding EDS of Fig. 5(a), (c) TEM image of VO<sub>2</sub> localized site, (d) corresponding EDS spectrum of Fig. 5 (c), (e) W localized site and the spot showing VO<sub>2</sub> and W hybridization (f) EDS and SAED pattern of the VO<sub>2</sub> and W hybridization spot.

Fig. 5 I-V characteristic curves of the VO<sub>2</sub> localized site (a) Heating cycle measurements from room to above transition and (b) Cooling cycle measurements from transition down to room temperature. (c) Temperature dependence Resistance measurements of the VO<sub>2</sub> site (a) from room to above transition and (d)  $\ln(\sigma T)$  against  $1/T$  of VO<sub>2</sub> site for heating and cooling cycle measurements.

Fig. 6 Electron Spin Resonance spectra of the VO<sub>2</sub> film (a) spectra for heating cycle measurement (b) spectra for cooling cycle measurement and (c) M vs H curve for the film



obtained from Vibrating Sample Magnetometry (VSM). (d) (inset) M vs H curve for pure VO<sub>2</sub> samples (e) (inset) M vs H curve for present thin film.

Fig. 7 Thermochromic hysteresis measure as inverse of ESR intensity against temperature for (a) 151.2 mT and (b) 308.7 mT peaks. Derivative of the magnetic susceptibility for (c) 151.2 mT heating data and 151.2 mT cooling data and (d) 308.7 mT heating data and 308.7 mT cooling data. In all a transition at 340 K is evident.

Figure 1

Fig 1

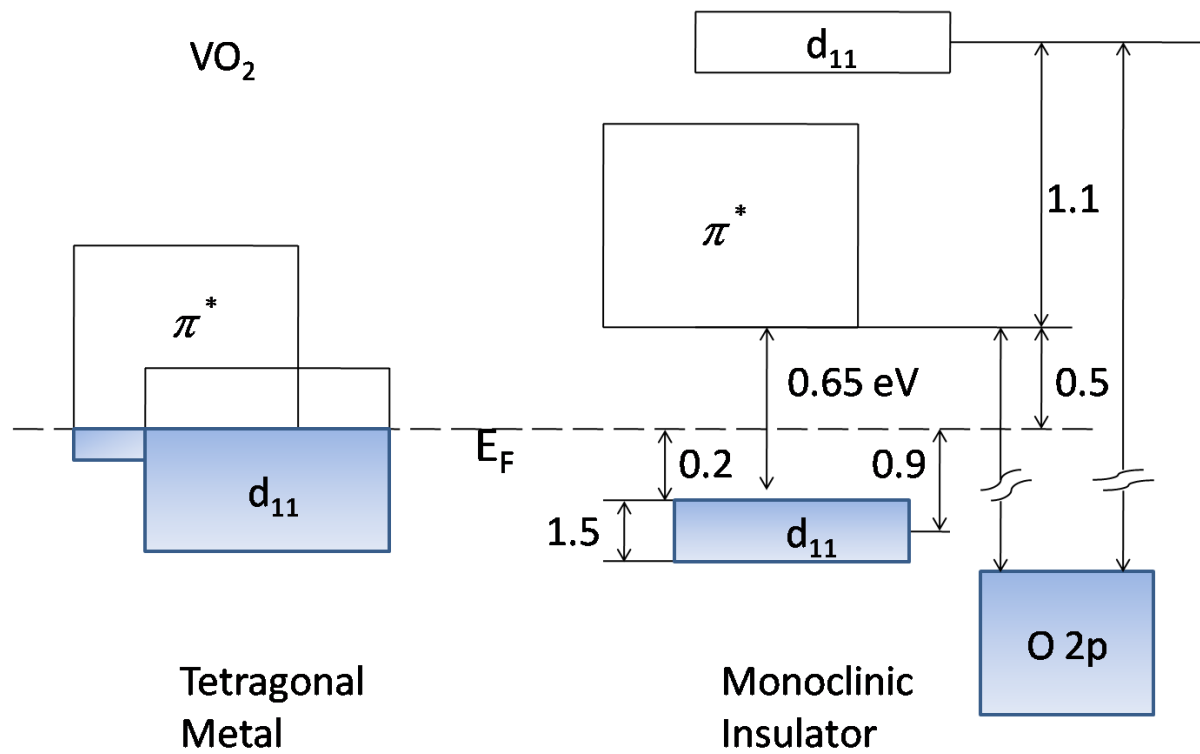


Figure 2

Fig 2

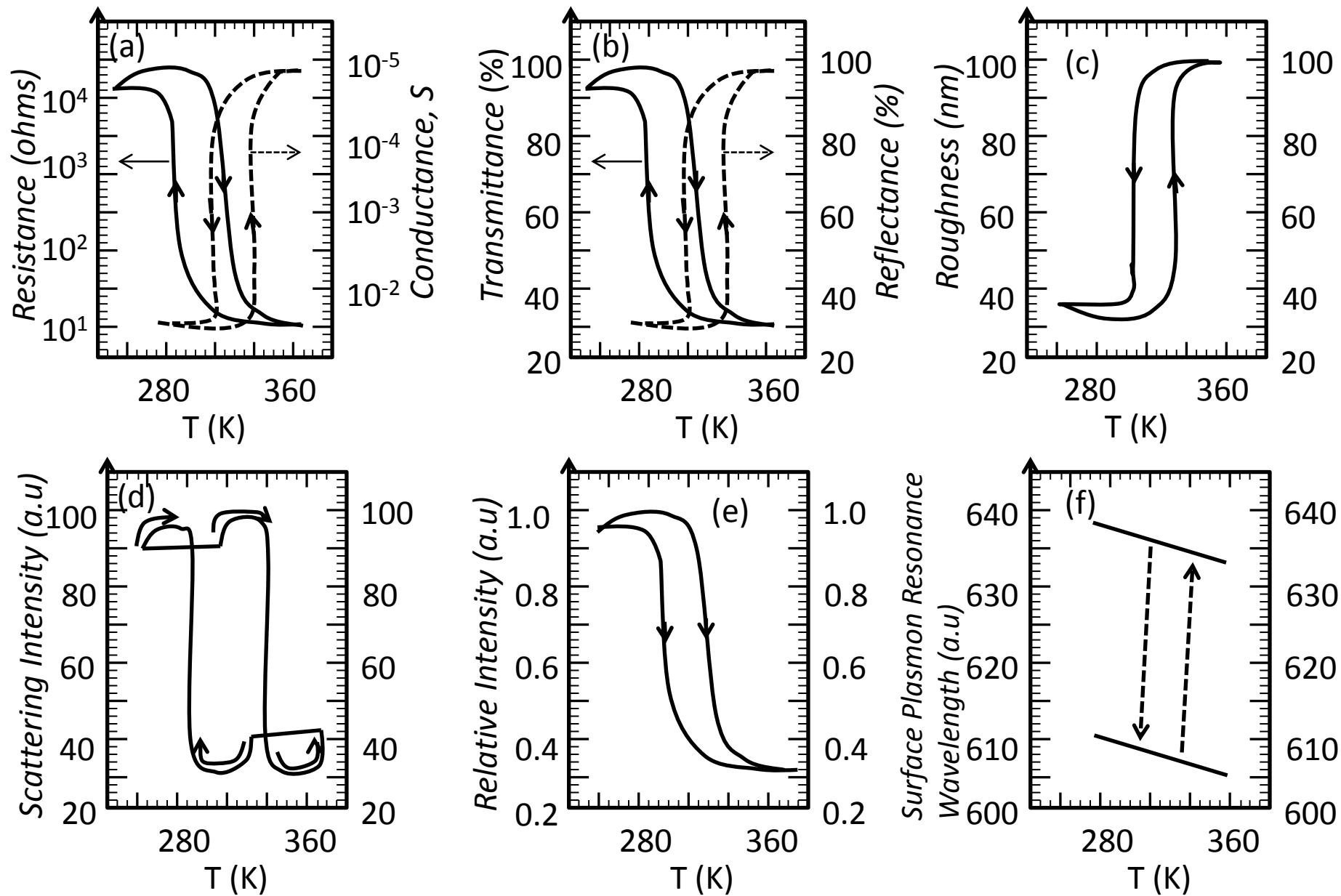


Figure 3

Figure 3

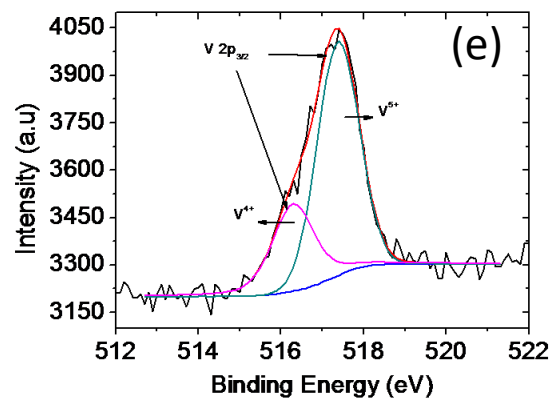
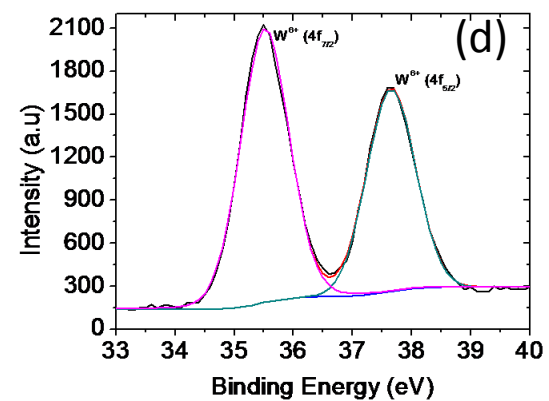
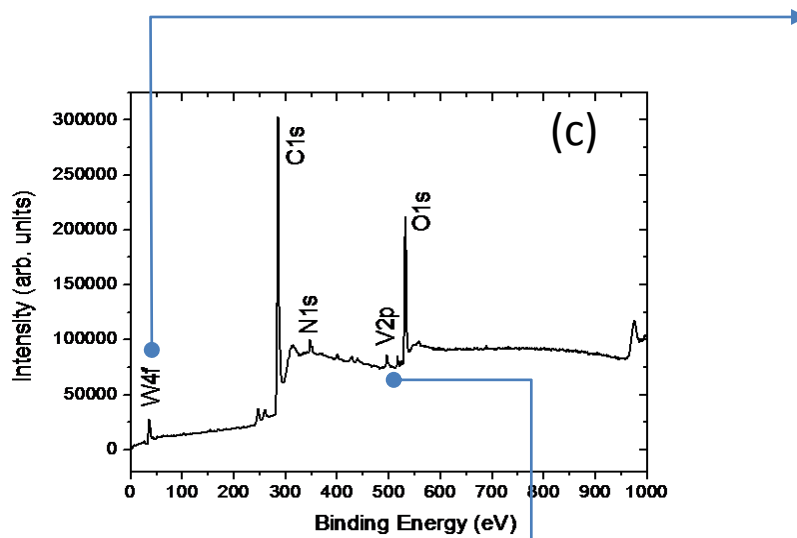
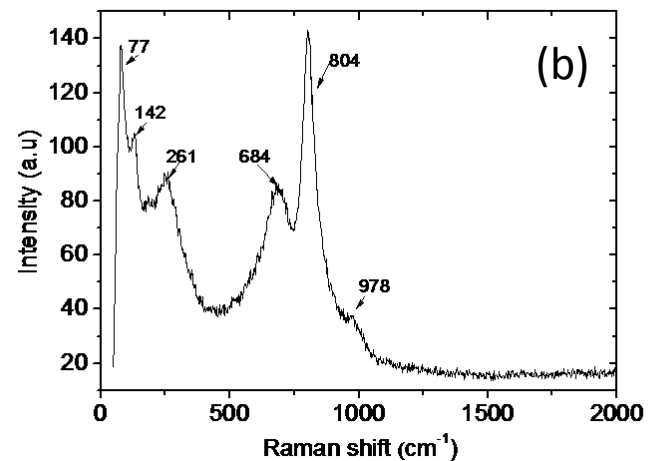
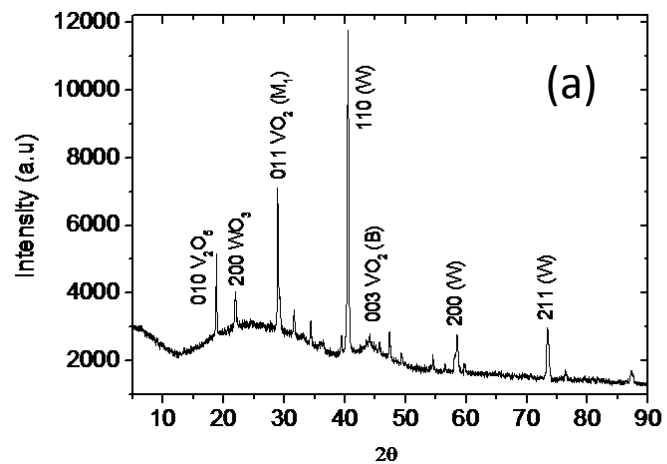


Figure 4

Fig 4

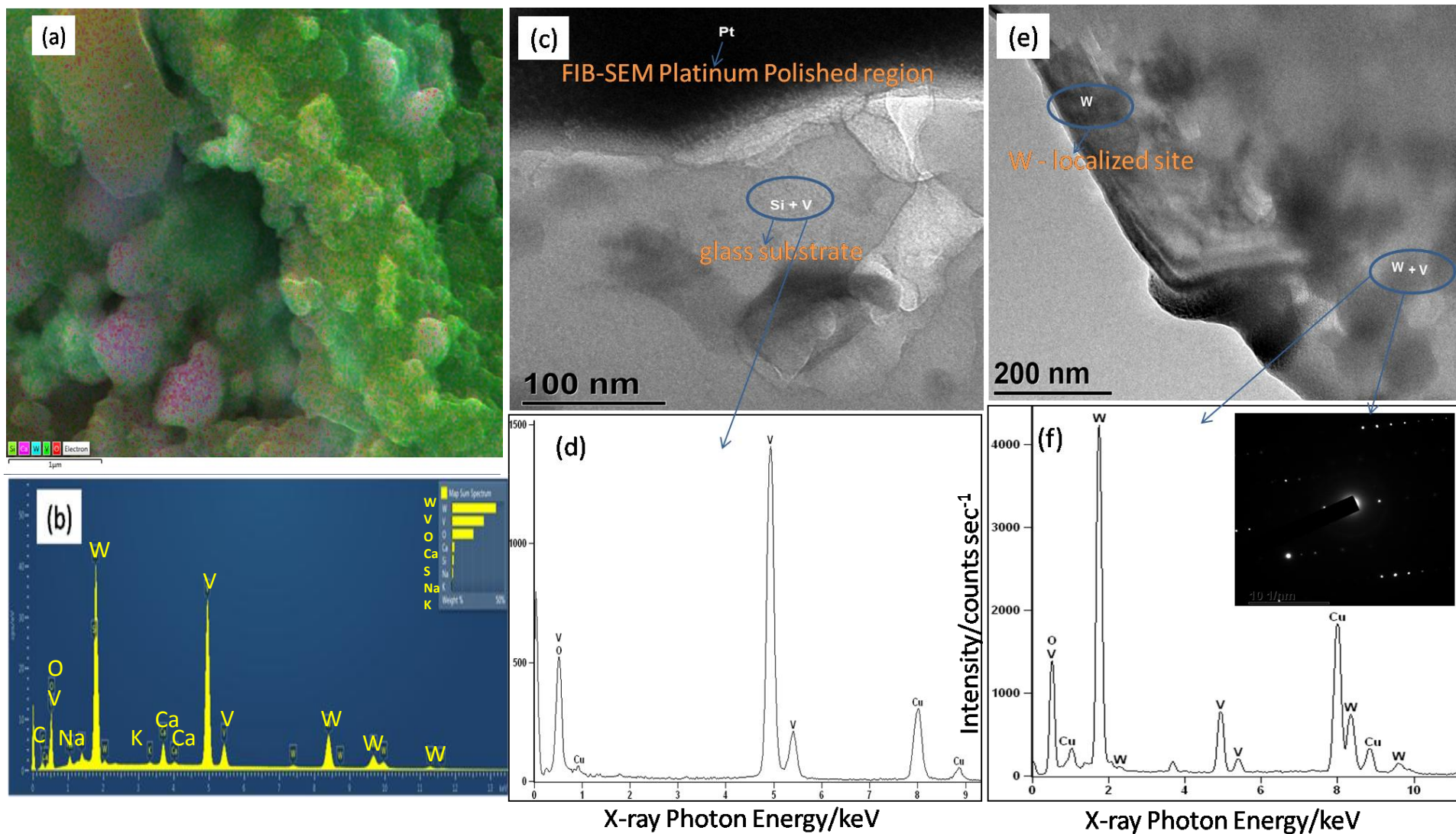


Figure 5

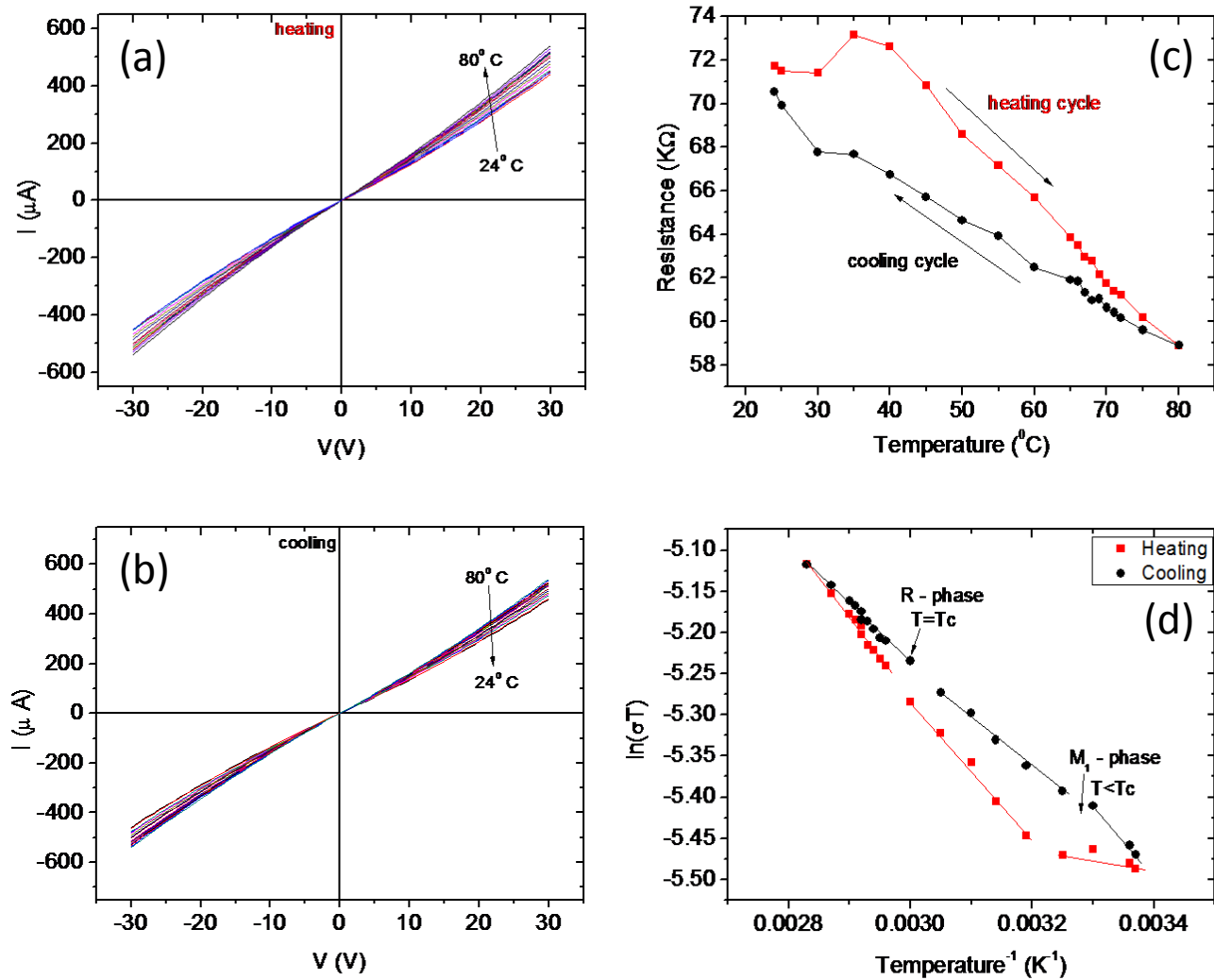


Figure 6

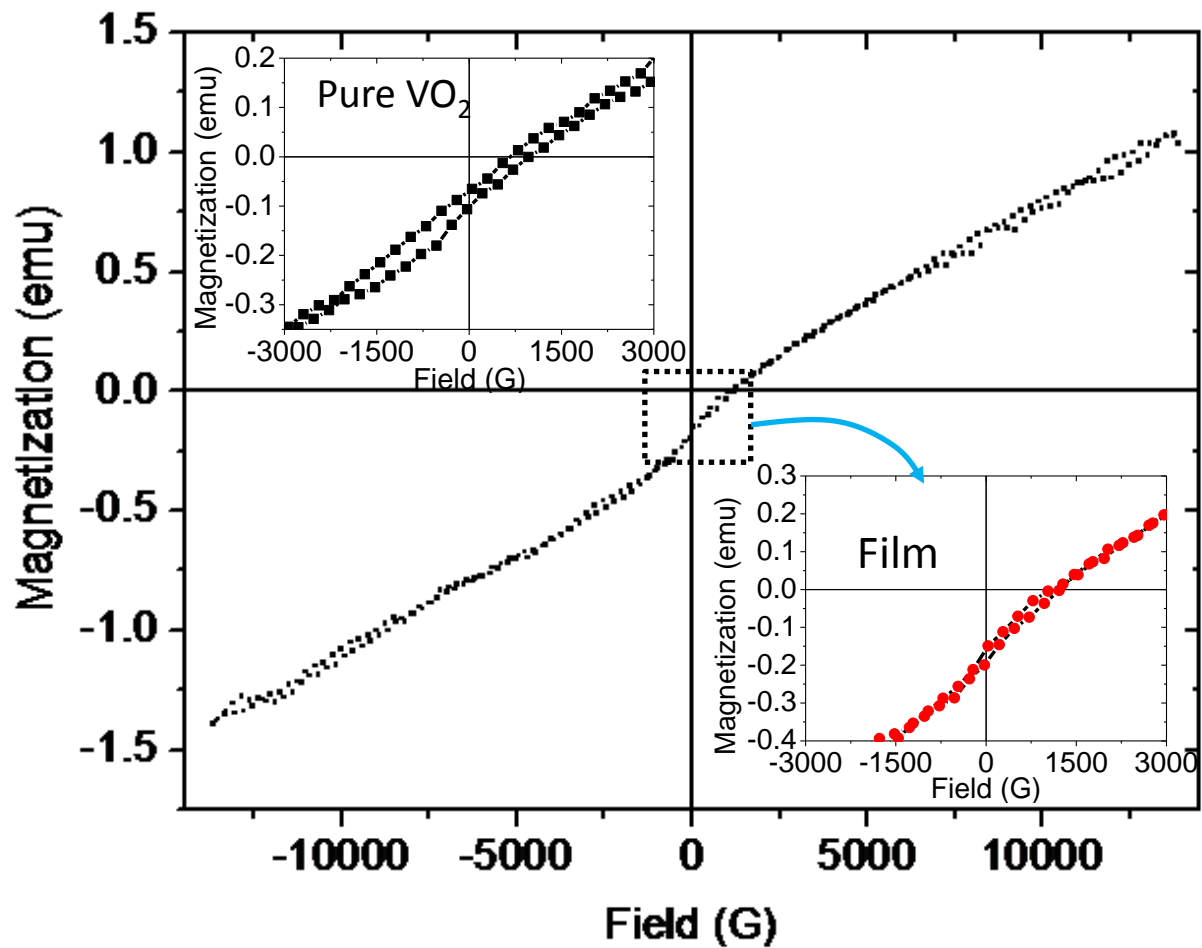
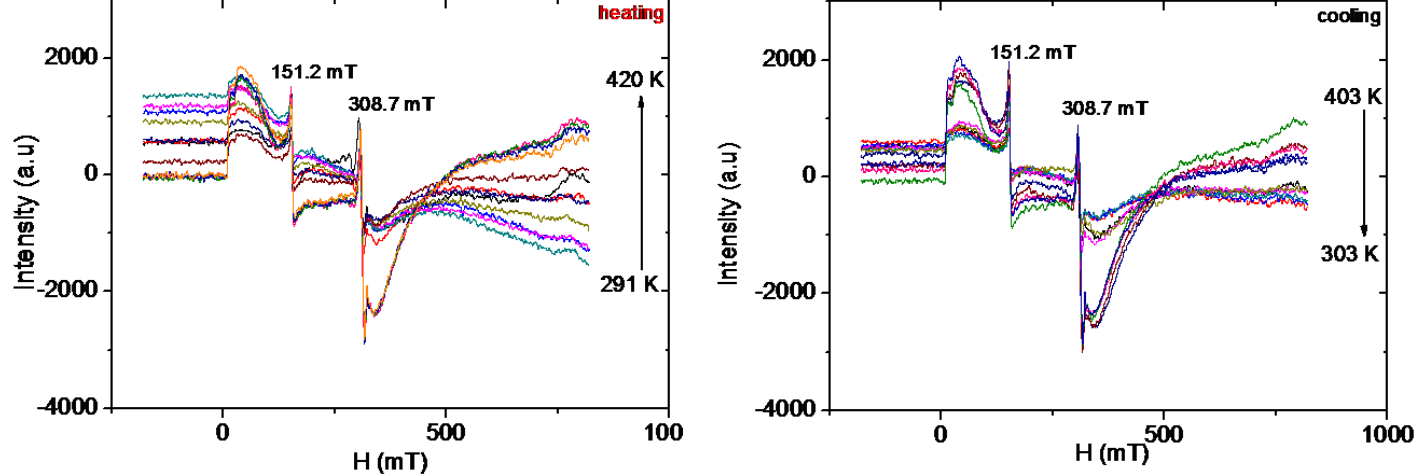


Figure 7

